High temperature fatigue behavior of notched Inconel 825 steel under constant amplitude and two step loading

Prakash Chandra Gope and Chetan Singh Mahar

College of Technology, Mechanical Engineering Department, G B Pant University of Agriculture and Technology, Pantnagar-263145, Uttarakhand, India

E mail: pcgope@rediffmail.com, pcg.fme@gbpuat-tech.ac.in

Phone: +91 9411159916 fax: +91 5944 233338

Abstract

In the present investigation temperature dependence fatigue strength behaviour of Inconel 825 super alloys is investigated. Based on the experimental results different S-N models have been derived and suitable model for the prediction of fatigue strength have been proposed. An inverse power and exponential relation between fatigue strength and absolute temperature is demonstrated. The proposed models are used to predict the fatigue life using well known Palmgren-Miner rule. Based on high to low and low to high load steps test data sets under identical test conditions, Miner rule based statistical damage constant is stochastically modeled for fatigue life prediction at different level of probability and validated. The modeling process combines a probabilistic fatigue damage accumulation and a stress-life-temperature relation technique.

Keywords: high cycle fatigue; S-N curve; variable amplitude loading; cumulative damage; probability

Nomenclature

ξ	Probability level
$\boldsymbol{\alpha}$, $\boldsymbol{\beta}$	Weibull probability distribution parameters
r	Correlation coefficient
M	Bending moment
D	Specimen diameter

σ_0 Bending stress

K_f Fatigue reduction factor

q Notch sensitivity

K_t Stress concentration factor

σ_a Stress amplitude

N_f Fatigue life

n Fraction of fatigue life or number of cycles applied at stress level σ

1.0 Introduction

The prediction of fatigue life under different loading condition is still an empirical art rather than a science. S-N curve approach first discovered by Wöhler in 1860 is still considered to be the most convenient approach by most of the designers in fatigue life prediction. Thereafter, different empirical models are frequently used by many researchers and designers for the fatigue life prediction. Among all such models Basquin model [1] is mostly preferred for modeling S-N data. Latter on various effects such as mean stress effect, notch, dimension, roughness, temperature, etc. on the S-N curves of Wöhler nature have been studied and included. These can be seen in the review work of Suresh [2]. Bending fatigue tests have been a field of immense interest from past several years for constructing S-N curves and a lot of researchers are working in this area. A large majority of work on bending fatigue concerning low cycle to very high cycle fatigue tests at room to high temperature are seen in the literature due its adequately representative of service loading in various rotating components [3-9]. Though the fatigue loading during service life of any machine component is very uncertain and have a combination of constant and random nature of peaks and valleys, the constant and two step loading may be considered as a representative of several types of loading found during service life or can be simplified to step loading applying various techniques such as cycle counting techniques, rain flow counting method etc. discussed by researchers in the past. However, in the present work such techniques are not applied but loading histories are designed to represent the generality of practical applications.

Due to very high complexity in fatigue phenomena under constant or variable amplitude loading the empirical model are not suitable for reliability assessment. So the

probabilistic predictive model is of great importance. The stochastic fatigue life prediction models under variable amplitude loading are presented by many authors mainly based on linear or nonlinear fatigue damage accumulation and stochastic or probabilistic S-N curve representation [10-15]

Many standards approved Inconel 825 as a material for pressure vessel operating up to temperatures of 525°C (AS1210, AS4041), 538°C (ASME Boiler & Pressure Vessel Code, Sections I, III, VIII, IX, Cases 1936, N-188) due to its improved corrosion resistance. In the present investigation temperature dependence of fatigue curves of Inconel 825 are investigated and the statistical damage model for Inconel 825 is derived combining the stress-life-temperature relation and probabilistic fatigue damage accumulation rule. The proposed model is validated with the experiential results of Inconel 825 and its suitability for reliability based prediction of fatigue life under different given probability level is illustrated.

2.0 Material and Methods

In the present investigation Inconel 825 nickel-chromium-based super alloy is used to study the influence of temperature on the S-N beahaviour. Due to improved high temperature corrosion properties Inconel 825 can be used in the parts which are subjected to high temperature. It is therefore, the study of influence of temperature on fatigue properties is useful and can be applied in design of components working under such environmental conditions. The chemical composition of Inconel 825 round bar (UNS N0 8825) used in the present investigation and determined by energy dispersive spectrometer (EDS) process are presented in Table 1.

Table 1. Chemical composition of Inconel 825

Element	C	Si	Cu	Mn	Mo	Cr	Ni	Al	S	Ti	Fe
wt.%	0.05	0.5	2.25	1.0	3.10	21.5	42	0.2	0.03	1.2	22

The mechanical properties of Inconel 825 determined according to ASTM E8 [16] are presented in Table 2. The tensile tests are conducted on a servo controlled universal testing machine (ADMET, USA) under displacement control at 0.5 mm/min crosshead speed.

Table 2 Mechanical properties of Inconel 825

Properties	Mean value
0.2% offset yield strength, MPa	338.0
Ultimate tensile strength, MPa	662.0
Elongation %	45.0
Hardness (Rockwell)	155.0
Modulus of elasticity (E), GPa	196.0
Density , g/cm^3	8.4
Poisson's ratio	0.29

Fatigue tests are conducted on round bars. The smooth specimens were made from round bar of diameter 10 mm having a length of 210 mm. The round bars were cut into pieces having a length of 210 mm with the help of Electric Discharge Machining (EDM) wire cut machine and a circumferential notch was made in middle. The cutting tool used for making notch in the specimen was having a tip radius 0.76 mm and the tool angle of 69°. The tool depth was kept to be 2 mm. The line diagram and the actual photograph of the notched specimen are shown in Fig. 1(a-c). All fatigue tests are conducted under four point bending and fully reversed stress cycles at room temperature to elevated temperatures. All fatigue tests are divided into four groups. In group 1, tests are conducted under constant amplitude loading to establish the S-N curves at different temperatures. Four temperature levels are selected for this purpose. In the second group, two and three steps loading tests are performed. The results from group 2 are used for Miner rule modeling and determination of statistical properties of the damage constant and probabilistic cumulative damage modeling. The statistical properties are also used in the Monte Carlo simulation. Group 3 tests conducted under constant amplitude loading at different temperatures are used for validation of the stress-life-temperature models. The results of group 4 under two steps variable amplitude loading are used for validation of the probabilistic cumulative damage model. Experimental design of groups 1-4 are shown in tables 3-6 respectively. All specimens are fatigued until full rupture or failure and the numbers of cycles required for failure are noted for further analysis.

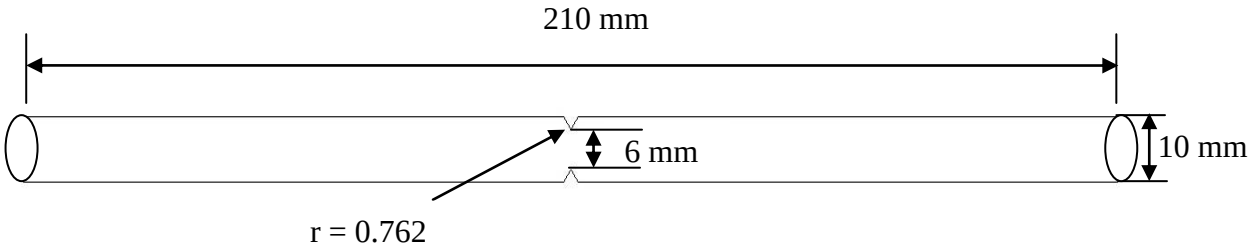

Fig. 1 (a) Line diagram of notch specimen

Fig. 1 (b) Photograph of notch specimen

Fig. 1 (c) Notched portion of the specimen

Table 3 Design of experiment for constant amplitude stress-life-temperature modeling

Stresses, MPa	600.6	500.0	360.0	240.5	90.7	60.5
Temperatures, K	303	473	573	773		

Note : Tests are conducted at 6 stress amplitudes and four temperatures

124 Table 4 (a) Design of experiment using Taguchi method for 3 step loading

Test No	Stress σ_1 (MPa)	Stress σ_2 (MPa)	Stress σ_3 (MPa)	T_1 (K)	T_2 (K)	T_3 (K)
1	167	167	167	303	303	303
2	167	167	167	303	573	573
3	167	167	167	303	773	773
4	167	250	250	573	303	303
5	167	250	250	573	573	573
6	167	250	250	573	773	773
7	167	417	417	773	773	773
8	167	417	417	773	303	303
9	167	417	417	773	573	573
10	250	167	250	773	303	573
11	250	167	250	773	573	773
12	250	167	250	773	773	303
13	250	250	417	303	303	573
14	250	250	417	303	573	773
15	250	250	417	303	773	303
16	250	417	167	573	303	573
17	250	417	167	573	573	773
18	250	417	167	573	773	303
19	417	167	417	573	303	773
20	417	167	417	573	573	303
21	417	167	417	573	773	573
22	417	250	167	773	303	773
23	417	250	167	773	573	303

24	417	250	167	773	773	573
25	417	417	250	303	303	773
26	417	417	250	303	573	303
27	417	417	250	303	773	573

Table 4 (b) Design of experiment for 2 steps loading

Load sequence	Stress, MPa		Temperature, K	No of replications
High-Low	417.0	250.0	573	27
Low-High	250.0	417.0	573	24

Table 5 Design of experiment for validation of stress-temperature-life model

Levels/tests	1	2	3	4	5
Stress levels, MPa (05)	600.6	360.0	240.5	90.7	60.5
Temperature levels, K (03)	473	573	773		

Table 6. Design of experiment based on Taguchi method and test results for validation of probabilistic cumulative model

Test No	Temperature (Kelvin)	Stress σ_1 (MPa)	n_1 (cycles)	N_1 (cycles)	Stress σ_2 (MPa)	n_2 (cycles)	N_2 (cycles)
1	303	167	50000	414529	417	34059	38269
2	303	250	45000	86127	417	21718	38269
3	303	417	25000	38269	167	85695	414529
4	573	167	15000	88486	417	5897	6698
5	573	250	27000	48968	417	3914	6698

6	573	417	4500	6698	167	20164	88486
7	773	167	14000	76125	417	3650	4017
8	773	250	15000	25435	417	2430	4017
9	773	417	3000	4017	167	17568	76125

The stress calculation under four point bending tests is made according to the following relation.

The nominal bending stress is calculated as:

$$\sigma_0 = \frac{32M}{\pi d^3} \quad (1)$$

where,

M = bending moment (N-mm)

d = notched specimen diameter (mm)

σ_0= nominal bending stress (MPa)

As the specimen is notched one the stress concentration factor should be applied to estimate the maximum stress or simply the localized stress as Eq. 2.

$$\sigma_a = K_t \sigma_0 \quad (2)$$

The stress concentration factor is defined as:

$$K_t = \frac{\sigma_{max}}{\sigma_{nominal}} \quad (3)$$

In Eq 3 σ_{max} is the local maximum stress (Eq 2) in the vicinity of the notch and the nominal is the nominal stress as defined by Eq 1. The theoretical stress concentration factor for notches in case of bending derived by Bader and Njim [17] is used here. These are presented in Eq. 4. The stress used in all cases here is the maximum stress level.

$$K_t = C_1 + C_2\left(\frac{2h}{D}\right) + C_3\left(\frac{2h}{D}\right)^2 + C_4\left(\frac{2h}{D}\right)^3 \quad (4)$$

for $2.0 \leq \frac{h}{r} < 50.0$,

$$C_1 = 0.965 + 1.926\sqrt{\frac{h}{r}}$$

$$C_2 = -2.77 - 4.414\sqrt{\frac{h}{r}} - 0.017\left(\frac{h}{r}\right)$$

$$C_3 = 4.785 + 4.681\sqrt{\frac{h}{r}} + 0.096\left(\frac{h}{r}\right)$$

$$C_4 = -1.995 - 2.241\sqrt{\frac{h}{r}} - 0.074\left(\frac{h}{r}\right)$$

(5)

where h is the notch depth, and r is the root notch radius and *D* is the specimen diameter. Taking $h = 2\ mm\ and\ r = 0.762\ mm$ values of C_1 to C_4 are computed and substituting the values of $C_1,\ C_2,\ C_3\ and\ C_4$ in Equation (5), we get, $K_t = 1.662$. Comparisons of fatigue test results for notched and un-notched specimens revealed that a reduced K_t was warranted for calculating the fatigue life for many materials [18-19]. As the specimen is notched one the fatigue stress reduction factor K_f is computed using the Eq. 6.

$$K_f = 1 + q(K_t - 1) \tag{6}$$

where q is the notch sensitivity. Under static loading within elastic limit stress concentration factor K_t is most suitable to compute the maximum stress at the notch tip or in front of notch, but in case of fatigue loading the fatigue reduction factor K_f is more suitable both under elastic and plastic state of stress. Thus, the maximum stress amplitude used to draw S-N curve is obtained from Eq. 7.

$$\sigma_a = K_f \sigma_{max} \tag{7}$$

The fatigue reduction factor is determined from the notch sensitivity factor and stress concentration factor. The notch sensitivity is taken as $q = 0.72$ [18], and hence the fatigue stress concentration factor is found from Eq. 6 as $K_f = 1.44$.

3.0 Fatigue life prediction models

The stress-cycles to failure are described by the Basquin equation (model 1) defined as:

$$\sigma_a = a(N_f)^b \tag{8}$$

where, a is the fatigue strength coefficient and b is the fatigue strength exponent. In the present work effect of temperature on the number of cycles to failure is shown by modifying the Basquin equation by assuming the temperature having a (i) power law effect (ii) exponential effect.

Considering temperature effect on the stress-life beahaviour, the modified Basquin equation is presented as:

$$\sigma_a = a\left(N_f\right)^b (T)^c \tag{9}$$

Taking log on both the sides we get,

$$log(\sigma_a) = \log(a) + blog\left(N_f\right) + clog(T)$$

$$log(\sigma_a) = a^* + blog\left(N_f\right) + clog(T) \tag{10}$$

where, c is a material constant and named as temperature sensitivity parameter, T is the temperature taken in Kelvin and a^* is substituted for $log(a)$. Equation (9) or (10) is named as model 2 in future discussion which is a linear logarithmic model used to incorporate the effect of temperature in the material.

Equation (11-12) named as model 3 which follows exponential law to incorporate the effect of temperature.

$$\sigma_a = a(N_f)^b \exp(cT) \tag{11}$$

Taking log on both the sides we get,

$$log(\sigma_a) = a^* + blog\left(N_f\right) + cT \tag{12}$$

3.1 Two Step Cumulative Fatigue Damage Modeling

Cumulative fatigue damage analysis plays a vital role in predicting fatigue life of components. More than 95 years ago, Palmgren suggested the concept of damage accumulation in 1924. The mathematical expression of the damage accumulation due to variable amplitude loading was given by Miner in 1945. After that different models have been proposed by researchers to determine the cumulative fatigue damage. A survey of cumulative damage models can be seen in the work of Fatemi and Vangt [19]

Mathematically the Palmgren-Miner rule is expressed as [20]

$$\sum \frac{\mathrm{n}}{\mathrm{N}} = 1 \tag{13}$$

For two step block loading, the Palmgren-Miner rule (Eq. 13) is written as:

$$\frac{n_1}{N_1} + \frac{n_2}{N_2} = 1 \tag{14}$$

where, $n_1, n_2 =$ applied cycles at load level $\sigma_1 \; and \; \sigma_2$ respectively and $N_1 \; and \; N_2$ are fatigue life at a load level $\sigma_1 \; and \; \sigma_2$ respectively. In general for multistep loadings the Miner rule is written as

$$\frac{n_1}{N_1} + \frac{n_2}{N_2} + \frac{n_3}{N_3} + \cdots \ldots \ldots \ldots \ldots = 1 \tag{15}$$

where, $n_i,$ applied cycles at load level σ_i and N_i is the fatigue life at a load level σ_i . In Miner rule critical damage taken as one is unsafe for many applications. This is because unity is considered on the assumption that fatigue damage corresponding to each stress cycle of a variable amplitude loading sequence is the same as that due to the same stress cycle under constant amplitude loading. However, the studies on the step loading or variable amplitude loading indicate that loading sequences are more damaging in nature than constant amplitude loading. The available results [21-30] provide qualitative information of influence of different parameters of the variable amplitude loading on the fatigue strength. The approach used by the researchers in the past studies is qualitative in nature and does not reveal any randomness in the S-N curve variables as well as in the critical damage sum. It has been reported that the right side constant (unity) in Miner rule varies from 0.78 to 2.7 [18] and thus Palmgren-Miner rule in many situations differs from Eq. 13. From the available experimental data, it can be observed that the summation of

damage fractions is either greater than unity or less than unity. From the experimental results it is seen that the material damage parameter called Palmgren-Miner damage constant $c > 1$ for Low-High (L-H) load level test and $c < 1$ for High-Low (H-L) load level test. So rewriting the Miner damage rule as:

$$\frac{n_1}{N_1} + \frac{n_2}{N_2} = c \tag{16}$$

where, '*c*' is the material parameter called Palmgren-Miner damage constant. Mostly, researchers use constant *c* as a deterministic manner as its value is influenced by several factors such as loading, surface conditions, welded or non-welded conditions, kind of material etc.. Due to associated uncertainties in the influencing parameters the deterministic constant *c* may be treated as a random variable. Generally base line S-N curves are adopted for the Miner damage calculation by the researchers. These base line S-N curves are mean curves with 50% probability. If such practice is adopted than the assumption of *c* as random variable may not be sound. Hence, one way to consider c as stochastic nature, the Minor damage calculations has to be made from different probabilistic S-N curves. The assumption of stochastic of *c* may be sound enough if the tests are conducted under similar test conditions and the damage constant should be computed. There is another argument of considering damage constant c as scholastic or statistical in nature. The assumption of damage constant *c* as a statistical parameter rather than a deterministic parameter is true as the fatigue life *N* has probability characteristics, and thus *n* should have a probabilistic characteristics and the sum of the ratio of *n* to *N* is correspondingly statistical rather than deterministic. In recent years, probabilistic modeling of the damage rule has been proposed to describe the statistics of fatigue life and damage under constant and variable amplitude loadings. The statistical interpretation of Miner's rule from a probabilistic aspect by Birnbaum et al. [31], p–S–N curves and Miner's rule [32] or p–S–N curves and Markov chain models [33] to analyze the fatigue reliability for two-step fatigue tests, with both lognormal and Weibull distribution assumption of fatigue life are some of the studies found in the literature which concerned on the probabilistic aspect of Miner rule. From the above discussions and results of several researchers the damage parameter *c* is of statistical nature and it should be better treated statistically. In the present investigation, three probability distribution namely normal distribution, Weibull distribution and type I extreme value distribution are used to model *c*. It is found from the Goodness of fit results that the damage parameter *c* fits well

with all three distributions studied here. Two or three parameters Weibull distribution is one of the most widely used lifetime distributions in reliability engineering due to its versatility to take on the characteristics of other types of statistical distributions, in the present investigation the damage model parameter *c* is assumed to be Weibull distributed. Assuming the damage constant *c* as two parameters Weibull distributed, for the given probability of failure ξ, the damage parameter *c* can be estimated from:.

$$c_\xi = \alpha(ln\frac{1}{1-\xi})^{\frac{1}{\beta}} \quad (17)$$

where, **α** and **β** are Weibull parameters known as scale and shape parameters respectively.

Thus, the probabilistic model of the Palmgren-Miner rule for two step loading is written as:

$$\frac{n_1}{N_1} + \frac{n_2}{N_2} = \alpha(ln\frac{1}{1-\xi})^{\frac{1}{\beta}} \quad (18)$$

The fatigue life prediction can be obtained from Eq. 19.

$$\frac{n_2}{N_2} = \alpha(ln\frac{1}{1-\xi})^{\frac{1}{\beta}} - \frac{n_1}{N_1} \quad (19)$$

The validity of the proposed model is discussed in results and discussion section.

4.0 Results and Discussion

4.1 S-N curve for notched specimen

The notched specimens of Inconel 825 were tested on four point rotating bending fatigue testing machine at a frequency of 30 Hz and stress ratio $R = -1$ under constant amplitude loading. The tests were conducted at room and elevated temperatures. Minimum of three samples were tested at each condition. The results are summarized as S-N curve in Fig. 2. The S-N curve has been drawn between stress amplitude σ_a and fatigue life, i.e. cycles to failure N_f in log-log scale. The S-N curves plotted in Fig. 2 exhibit steep curves in the high cycle regime (>10^4 cycles) and slightly lesser steep in the low cycle regime (< 10^4 cycles). In the present test three stresses 600.6 MPa, 500 MPa and 360 MPa are higher than yield strength (under room temperature) of the material.

Thus, these stress levels produce elastic-plastic stress states at the notch, which appears to be reason for the bended curve in the low cycle fatigue regime with different slopes than at the high cycle zone. This indicates that single log-log straight line over the full range of stress levels is not accurate.

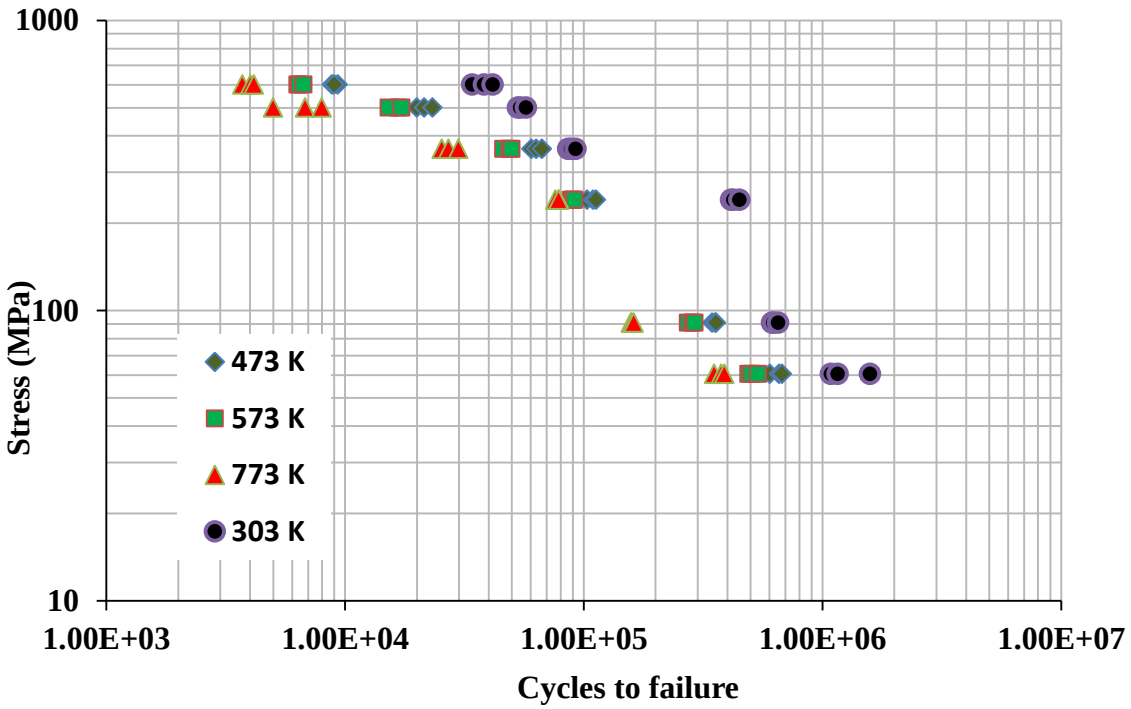

Fig. 2 S-N curves of Inconel 825 at different temperatures

Based on the experimental data, regression parameters of Eq. 8, 9 and 11 are obtained and results are presented in table 7 and 8 for low cycle as well as high cycle zone. i.e for elastic and plastic zones.

Table 7 Parameters of Basquin model (Equation 8)

Temp. (K)	Frequency (RPM)	Stress Ratio (R)	a	b	r	Condition
303	2700	-1	5.0×10^8	-1.145	0.811	Applicable

473	2700	-1	2.0×10^6	-0.779	0.995	for $\sigma < \sigma_y$
573	2700	-1	2.0×10^6	-0.802	0.996	
773	2700	-1	4.0×10^6	-0.869	0.922	
303	2700	-1	314275.0	-0.593	0.963	Applicable for $\sigma \geq \sigma_y$
473	2700	-1	6736.7	-0.264	0.987	
573	2700	-1	5758.8	-0.256	0.984	
773	2700	-1	4648.7	-0.251	0.966	

Table 8 Parameters of different proposed models

Model	a	b	c	r	Limiting condition
Model 2	2.728×10^8	-0.680	-0.975	0.909	$\sigma < \sigma_y$
	2.496×10^5	-0.272	-0.570	0.950	$\sigma \geq \sigma_y$
Model 3	9.995×10^6	-0.805	-0.00239	0.930	$\sigma < \sigma_y$
	1.243×10^4	-0.271	-0.00105	0.943	$\sigma \geq \sigma_y$

The derived predicted models given in Equation (8-11) are validated through the sets of fatigue data obtained under the test conditions mentioned in Table 5 and shown in Fig. 3-5. The validated test data are different than the dataset used in modeling.

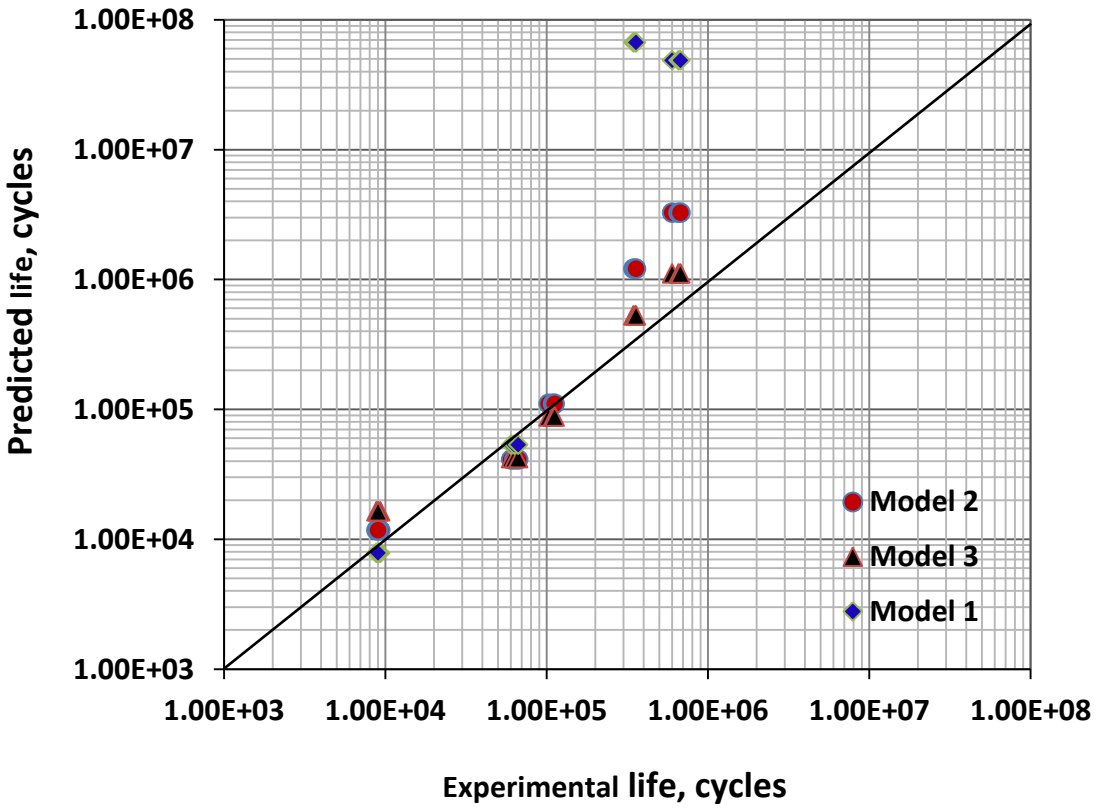

Fig. 3. Validation of stress-life-temperature models for Inconel 825 at 473 K

Fig. 3 shows the experimental and predicted results for five stress levels ranging from 60 MPa to 600 MPa at 473 K. Three fatigue life predicted models are used for comparison. The Basquin model (model 1) fits well for stress levels $\sigma_a \geq \sigma_y$. The ratio of experimental to predicted life is found to be between 1.1 to 1.25 for $\sigma_a \geq \sigma_y$ and the variation is about 30 to 60% for $\sigma_a < \sigma_y$. It is found that the predicted results for applied stress $\sigma \geq$360 MPa remained within 2% which increased to about 60% when the stress level is 60 MPa. Hence, at the low stress amplitude Basquin model is not suitable at 473 K. The ratio between the experimental and predicted fatigue life from model 2 and model 3 are found to be varied from 0.75 to 1.6 and 0.5 to 1.5 respectively. Model 3 predicts within less than 7% error for all range of stress amplitude. From the results summarized in Fig. 3, it can be observed that the predicted model 3 fits best with the experimental data for elastic and plastic ranges of stress amplitudes. It should be noted that the error is calculated on the basis of log values of experimental and predicted number of cycles to

failure. Fig. 4 shows the validation results at 573 K. Similar qualities of predicted results are seen at 573 K by all three models. However, the ratio of experimental to predict results are found to be varied between 1.2 to 2.5 for higher stress amplitudes and the percentage difference remained within 10% for all ranges of stress. This shows that quality of prediction improved for higher temperature. It is also seen that exponential model of temperature effect (model 3) predicts the results within 7% for entire ranges of stress. This percentage reduced to about 4% when the stress level is kept $\sigma \leq 240$ MPa. The prediction quality improves more for higher temperature level of 773 K as shown in Fig. 5. The ratio of experimental to predicted life is found to be between 0.9 to 3.4 , 0.3 to 2.0 and 0.63 to 1.5 for model 1, model 2 and model 3 respectively. It can be seen that the overall prediction for all ranges of temperature and stress levels by model 3 is better as compared to other two models. When the predicted results are critically analyzed, it is seen that model 2 predicts the fatigue live over the entire ranges of stresses studied here with percentage difference of 0..8 to 12.7, 1.5 to 11.4 and 0.02 to 9.3 for temperatures of 473 K, 573 K and 773 K respectively. The corresponding % errors obtained with model 2 are 1.3% to 4.6%, 2% to 7% and 0.2% to 8%. The results reveals that model 3 is better than model 2. For stress level $\sigma \geq 360$ MPa, model 2 predicts within 2.5 to 4.3% error, 1.75% to 5.5% error and 0.02 % to 6.9% error for 473 K, 573 K and 773 K respectively whereas the corresponding percentage error are 0.08 to 12.7, 1.65 to 11.4 and 6 to 9.3 for $\sigma < 360$ MPa. The percentage error between the experimental and predicted fatigue life by model 3 for stress level $\sigma < 360$ MPa are 1.4 to 4.6, 2.0 to 3.6 and 0.2 to 8.0 for 473 K , 573 K and 773 K respectively while the model 2 predicts with a percentage error of 0.08 to 12.7, 1.6 to 11.4 and 6.0 to 9.3 for 473 K , 573 K and 773 K respectively. The results reveal that higher quality of prediction is obtained by model 3 at higher temperature as compared to model 2 for entire ranges of stresses studied. If the predicted results are compared for 473 K, model 2 predicts better results than model 3 for entire ranges of stress amplitudes. The prediction quality continues for temperature level 573 K and stress level $\sigma \geq 360$ MPa but as the testing temperature exceeds 573 K model 3 seems to be superior with less predicted error than other two models. The temperature effect in model 2 and 3 are modeled as power law and exponential law respectively. Better predicted results for temperature $T \geq 573$ K by model 3 indicate that the fatigue life follows exponential relation between stress amplitude and temperature.

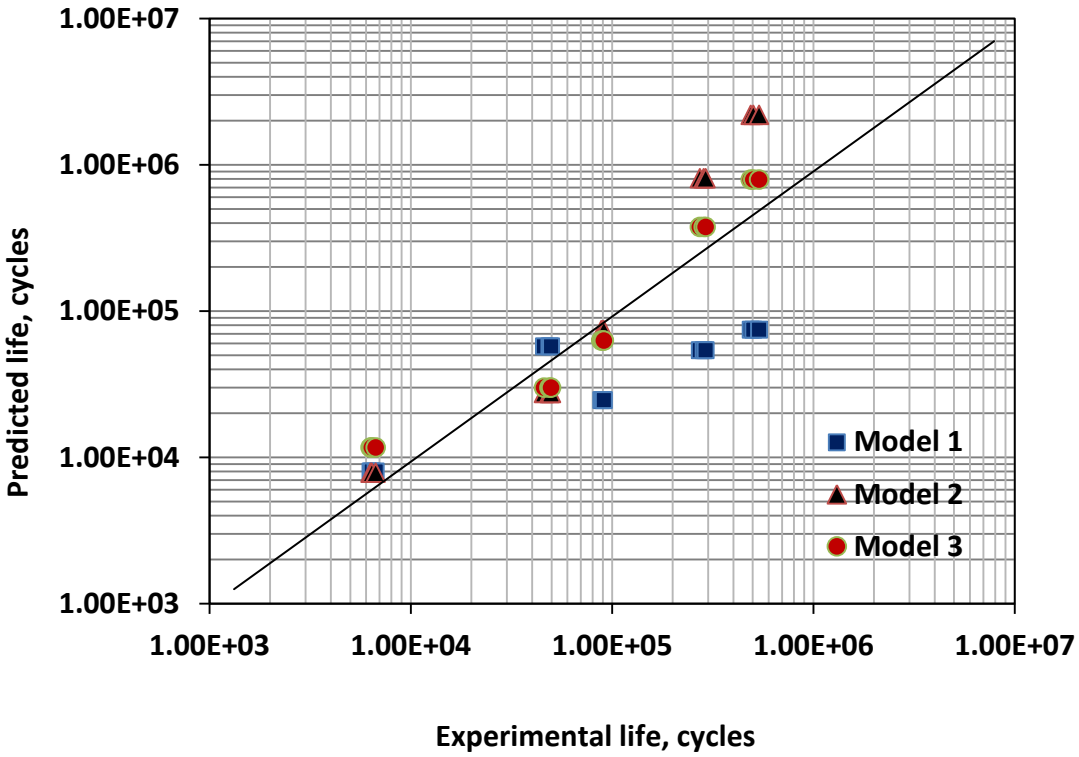

351

352 Fig. 4 Validation of stress-life-temperature models for Inconel 825 at 573 K

353

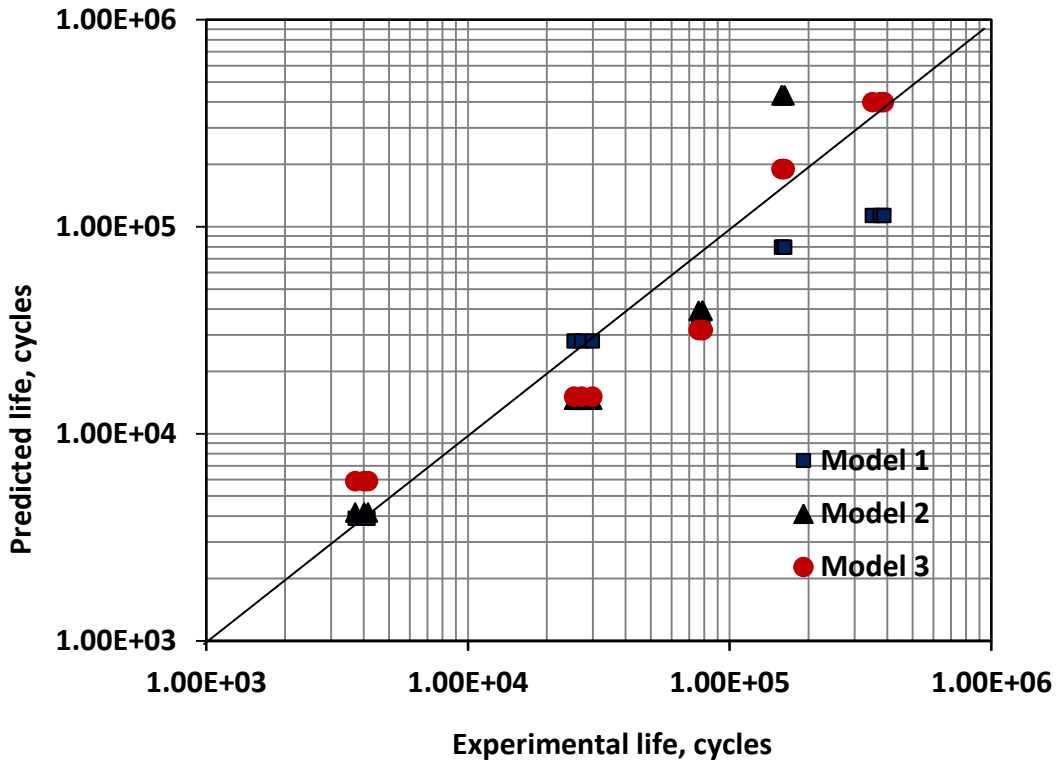

354

355 Fig. 5 Validation of stress-life-temperature models for Inconel 825 at 773 K

From the above observations in Figs 3-5 it can be concluded that no single model is suitable for entire range of the stress level. A bend curve or two separate straight line fitting seems to be more appropriate than a single straight line fitting. The elastic-plastic range at notch which appears to be the reason for the bended curve from the elastic zone seen in Fig 3-5 or the development of elastic-plastic zone at higher stress or at higher temperature at notch may be the reason of the higher scatter in the data in elastic-plastic zone. Hence, single log-log predicted model or other form of predicted model over entire range of stress levels fails to predict with a reasonable accuracy. Fig. 3-5 also reveals that predicted line with 50% probability (as all are based on mean values) is not suitable in reliability assessment. Hence, lower and upper bound predictive models are required to address these issues.

4.2 Two step or variable amplitude loading

In order to find the probability distribution and the statistical parameters of *c*, two sets of two step tests are conducted for two type of load sequences low to high (L-H) in the first set of experiment with 24 replications and high to low (H-L) in second set of experiment with 27 replications. Special care is taken for identical sample preparation for all tests. The loading parameters used in low to high and high to low are 250 MPa, 417 MPa and 417 MPa, 250 MPa at 573 K respectively. Number of load cycles obtained in two step tests is used to calculate damage parameter *c*. According to Miner cumulative damage model (Eq. 16) the summation of the fraction yields the magnitude of *c*. Based on the experimental data, it is seen that the miner constant *c* varies from 0.8 to 1.05 in case of H-L loading and 0.92 to 1.25 in case of L-H load sequence. Treating the constant as random variable, normal probability distribution, Weibull and extreme value probability distribution function are determined. The different distribution parameters are presented in Table 9. The results of *c* are plotted as cumulative distribution function (CDF) in Fig. 6. CDF from normal distribution, Weibull and extreme value distribution, r^2 values are included in the table 9.

383

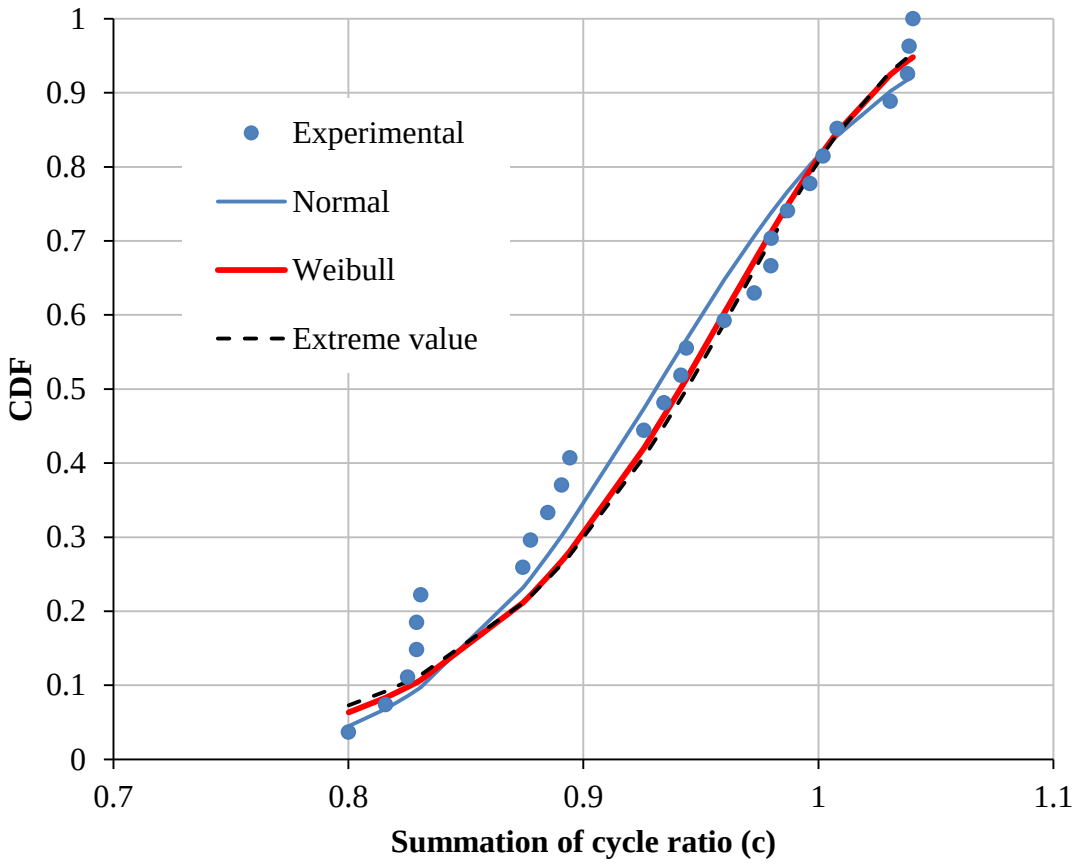

384

385 Fig. 6 (a) Probability distribution of Palmgren-Miner rule damage parameter *c* for High to
386 low load sequence

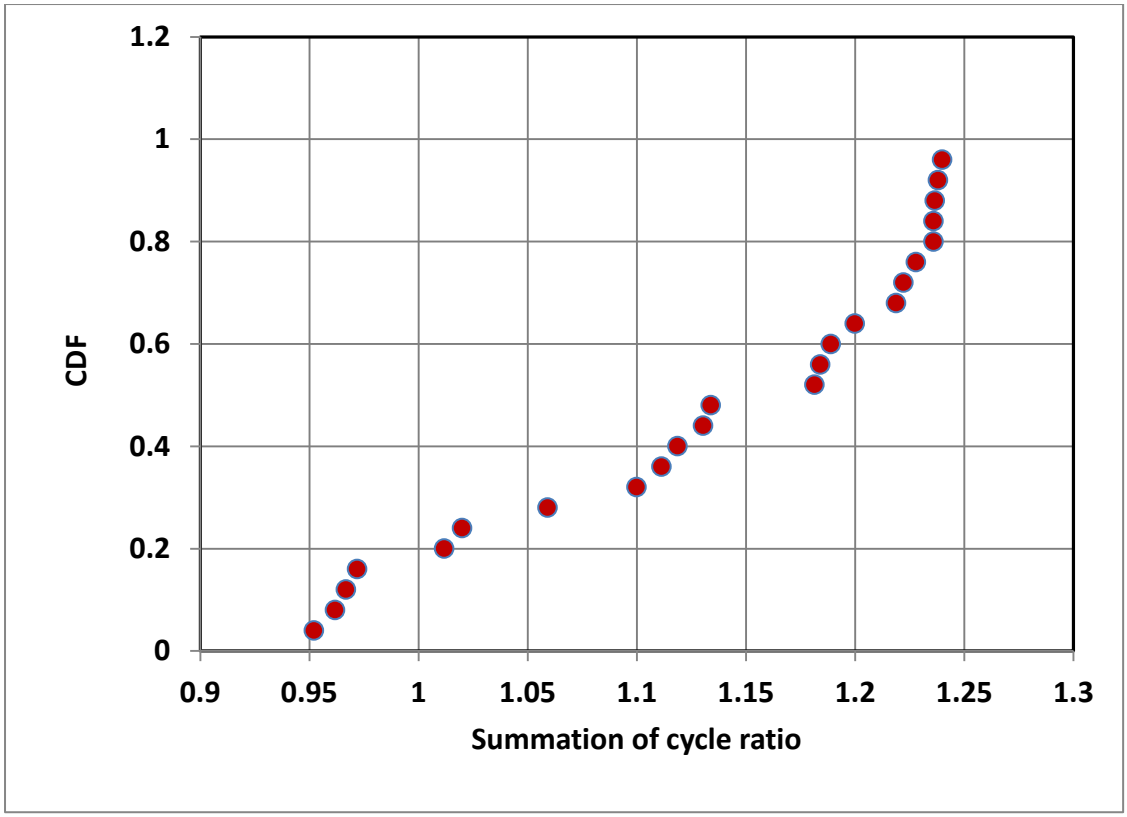

Fig. 6 (b) Probability distribution of Palmgren-Miner rule damage parameter *c* for Low to High load sequence

Table 9 (a) Statistical parameters of Palmgren-Miner rule damage parameter *c* and r^2value

Load sequence	Normal Parameters			Weibull Parameters			Extreme Value Parameters		
	μ	σ	r^2	α	β	r^2	δ	θ	r^2
H-L	0.930	0.077	0.966	0.965	14.513	0.966	0.967	0.064	0.965
L-H	1.131	0.108	0.961	1.177	14.425	0.961	1.180	0.077	0.960

Table 9(b) Kolmogorov-Smirnov (K-S test) statistics at 5% significance

Load sequence	Normal distribution	Weibull distribution	EV distribution
H-L	0.515	0.525	0.528
L-H	0.519	0.518	0.520

Fig. 6 represents the CDF plot of Palmgren-Miner rule constant, *c* using normal, Weibull and extreme value probability distribution. On comparing the experimental CDF plot for of Palmgren-Miner rule constant against the probability distribution curves the regression coefficient were found to be 0.966, 0.965 and 0.965 for normal, Weibull and extreme value probability distribution respectively for H-L load sequence using Equation (20) given by Doremus [34] as:

$$r^2 = 1 - \frac{\sum_{j=1}^{n}(x_j - \hat{x})^2}{\sum_{j=1}^{n}(x_j - \mu)^2} \tag{20}$$

where, *n* is the total number of data points,x_j is the j^{th} data point of the random variable that is ranked from smallest to largest, $\hat{x}$ is the calculated value from fitted distribution function at rank $F(x_j)$ and μ is the mean value. r^2 explains how well the regression represents the data. From the r^2 value, normal probability distribution or Weibull distribution is the most suitable followed by the type I extreme value probability distribution. The goodness of fit test by K-S statistics shown in table 9(b) also reveals the similar conclusion. However, from the mechanics of the fatigue failure, Weibull distribution is more suitable for failure analysis. Hence, in the present investigation Weibull distribution is selected for reliability prediction model. However, the statistical results of all three distributions are presented for comparison in table 9(a-b). The Weibull distribution parameters are estimated from the 27 test results of Inconel 825 for High-Low load sequence using maximum likehood function are $\bar{a} = 0.965$ and $\bar{b} = 14.513$. and taken to illustrate the application and derivation of the probabilistic cumulative damage model as below.

$$\frac{n_2}{N_2} = 0.965\left(ln\frac{1}{1-\xi}\right)^{\frac{1}{14.513}} - \frac{n_1}{N_1} \tag{21}$$

To compute the upper and lower limit of the predicted life, the probability of failure ξ should be used as ξ or $1-\xi$ respectively. For example, for 90% probability level, the values of ξ are 0.90 and 0.1 for upper and lower bound of the predicted life. Eq 21 is suitable for prediction of fatigue life or remaining life when the requirement is limited to given probability. Fig. 7-9 shows the predicted results along with the validation data points at different probability using Eq. 21. In validation data all combination of loads are considered to illustrate the model capability.

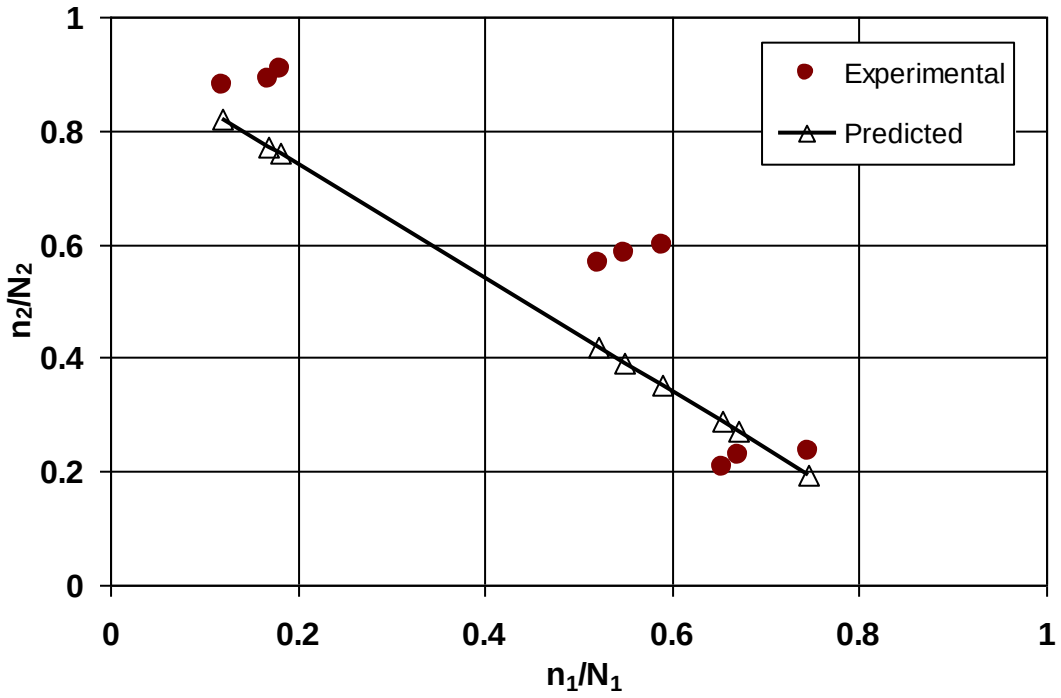

Fig. 7 Validation of the probabilistic cumulative fatigue damage model at 50% probability (validated data)

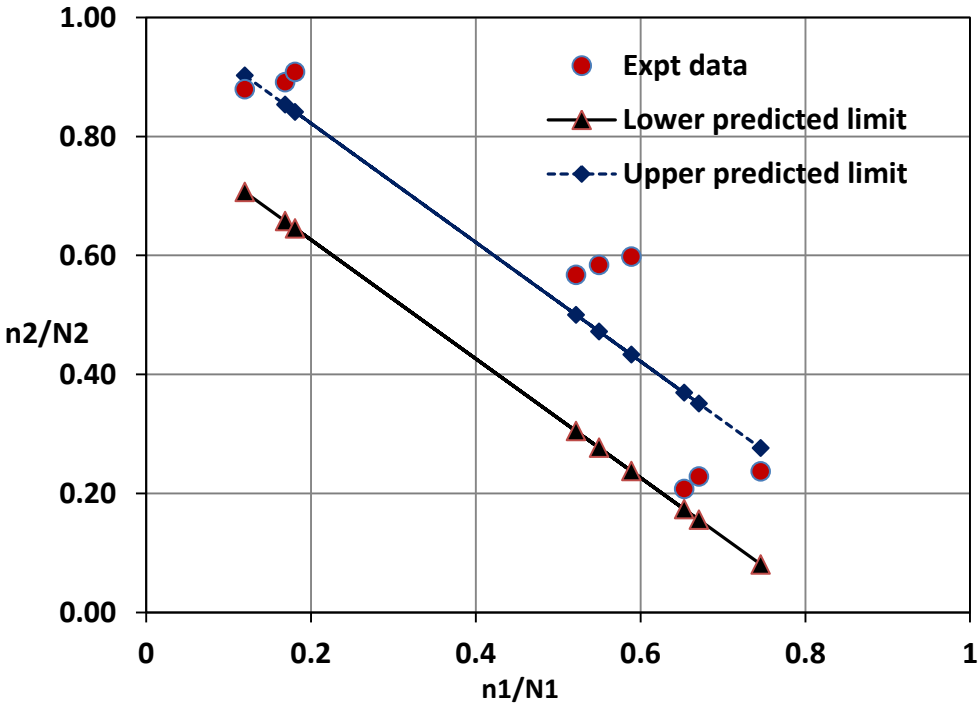

431

432 Fig. 8 Validation of the probabilistic cumulative fatigue damage model at 90%
433 probability (validated data)

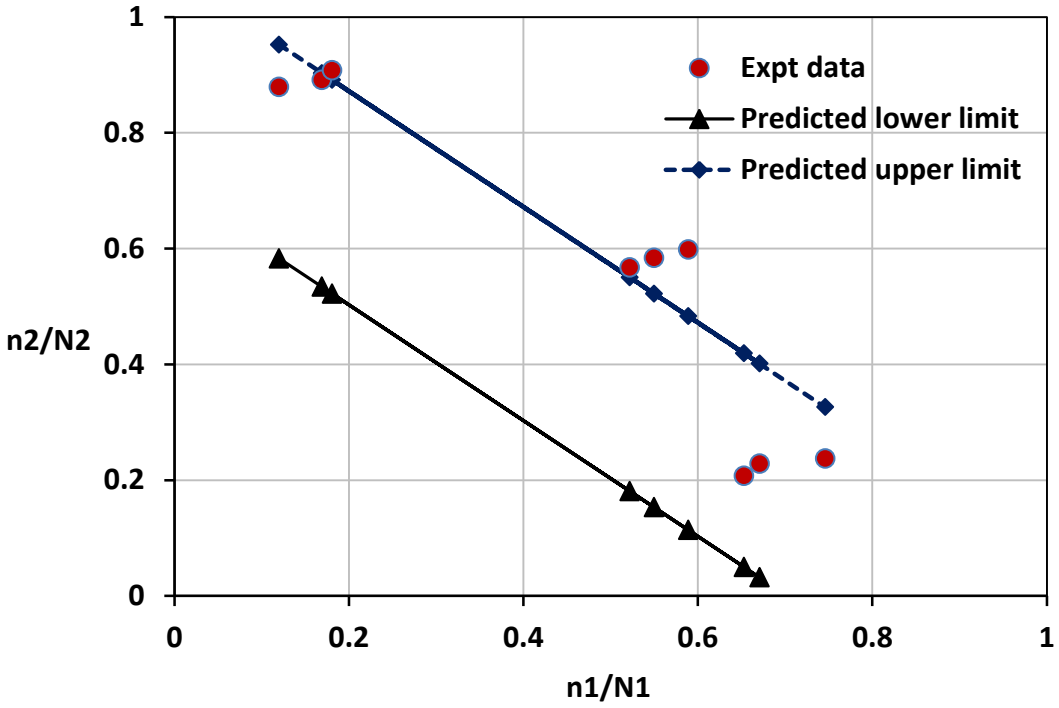

434

435 Fig. 9 Validation of the probabilistic cumulative fatigue damage model at 95%
436 probability (validated data)

Fig 7-9 illustrated the use of probabilistic approach to estimate the lower and upper limit of the predicted live for given probability of failure. Fig. 7 is plotted for 50% probability level. The predicted results shown in Fig. 7 indicate the mean curve of the experimental data. Fig. 8 and 9 are plotted for 90% and 95% probability level respectively. The figures reveals that about 45 % and 67% data are well within the two limits predicted by the proposed method for unknown dataset (i.e data not used for probabilistic modeling) at 90% and 99% probability. It is important to mention that the derived statistical parameter used in the validation are taken from H-L load sequence whereas in the validation both H-L and L-H load sequence at different temperature are considered. More study is required to find the distribution parameters of damage constant and their correlation with loading sequence and other loading parameters. The proposed method shows the importance of inclusion of probability into the cumulative damage model. Hence, it can be said that the fatigue life or the fraction of fatigue life predicted by proposed probabilistic cumulative damage model is found to be more suitable and shows that it is reasonably good to use in the reliability based design approach.

5.0 Conclusions

On the basis of experimental investigation of fatigue life of Inconel 825 at different temperature following conclusions can be drawn:

1. Power law modeling of the temperature effect is found to be more suitable at low temperature range and exponential modeling at higher temperature beyond 673 K.
2. From the stress temperature curve it was observed that the slope change effect is decreased for higher number of cycles to failure as compared to that of lower number of cycles to failure.
3. The experimental results under variable amplitude loading shows that summation of the life ratio is not unity as described in Palmgren-Miners rule, but it varies from 0.8 to 1.05 with a mean and standard deviation of 0.930 and 0.077 for High-Low load sequence and 0.92 to 1.24 with mean and standard deviation of 1.131 and 0.108 for low –high load sequence.
4. The constant is found to be random in nature and it most suitably fits to normal or Weibull probability distribution.

5. The probabilistic cumulative damage model presented in this work is more suitable to predict the fatigue life under variable amplitude loading at any desired level of probability. This can also be helpful for the reliability assessment of a component under variable amplitude loading.

References

[1] Basquin OH. Exponential law of endurance tests. Proc ASTM 1910;10:625-630.

[2] Suresh S. Fatigue of metals. Cambridge University Press; Cambridge 1998.

[3] Hüseyin Özdeş, Murat Tiryakioğlu, Paul D.Eason. On estimating axial high cycle fatigue behavior by rotating beam fatigue testing: Application to A356 aluminum alloy castings. Mater Sci Engng. A 2017; 697: 95-100.

[4] Berto, F., Gallo, P, Lazzarin P. High temperature fatigue tests of un-notched and notched specimens made of 40CrMoV13. 9 steel. Materials & Design. 2014; 63:609-619.

[5] Kohout, J., 2000. Temperature dependence of stress–lifetime fatigue curves. Fatigue & Fracture of Engineering Materials & Structures. 23(12): 969-977.

[6] R. R. Paulson, G. Fritzemeier, J. K. Tien, S-N Curve inversion of a nickel-base superalloy at elevated temperature. Metallurgical Transactions A March 1983;14(3):727–731.

[7] Kawagoishi N, Chen Q, Nisitani H. Fatigue strength of Inconel 718 at elevated temperatures Fatigue Fract Engng Mater Struct. DOI: 10.1046/j.1460-2695.2000.00263.x, 1999; 23:209-216

[8] Eleiche, AM., Megahed, MM. and Abd-Allah, NM. Low-cycle fatigue in rotating cantilever under bending. III: Experimental investigations on notched specimen Int J fatigue 2006; 28(3): 271-280.

491 [9] T.Hassan, Z.Liu. On the difference of fatigue strengths from rotating bending, four-
492 point bending, and cantilever bending tests, International Journal of Pressure Vessels and
493 Piping.2001;78(1):19-30.

494 [10] Liao M, Xu X, Yang QX. Cumulative fatigue damage dynamic interference
495 statistical model. Int J Fatigue 1995;17:559–66.
496 [11] Kam TY, Chu KH, Tsai SY. Fatigue reliability evaluation for composite laminates
497 via a direct numerical integration technique. Int J Solid Struct 1998;35:1411–23.
498 [12] Le X, Peterson ML. A method for fatigue based reliability when the loading of a
499 component is unknown. Int J Fatigue 1999;21:603–10.
500 [13] Shen H, Lin J, Mu E. Probabilistic model on stochastic fatigue damage. Int J Fatigue
501 2000;22:569–72.
502 [14] Davide Leonetti, JohanMaljaars H.H. (Bert) Snijder. Fitting fatigue test data with a
503 novel S-N curve using frequentist and Bayesian inference. Int J Fatigue;2017:105:128-
504 143.
505 [15] Luca D'Angelo, Alain Nussbaumer. Estimation of fatigue S-N curves of welded
506 joints using advanced probabilistic approach. Int J Fatigue 2017:9:98-113.
507 [16] ASTM E8 / E8M-16a, Standard Test Methods for Tension Testing of Metallic
508 Materials, ASTM International, West Conshohocken, PA, 2016, www.astm.org
509 [17] Bader Q, Njim, EK. Effect of stress ratio and v notch shape on fatigue life in steel
510 beam. Int J Scientific Engng Res. 2014;5(6): 1145-1154.
511 [18] Shigley, J. Mischke, C. Mechanical Engineering Design, Tata Mcgraw-Hill, Delhi,
512 5th ed. 310 p. 1989
513 [19] Fatemi A, Vangt L. Cumulative fatigue damage and life prediction theories: a
514 survey of the state of the art for homogeneous materials Int. J. Fatigue 1998;20(1):9-34.
515 [20] Miner MA. Cumulative damage in fatigue. J Appl Mech 1945;67:A159–A164.

516 [21] Fisher JW., Nussbaumer, A., Keating PB., Yen BT. Resistance of Welded Details
517 Under Variable Amplitude Long-Life Fatigue Loading, Tech. rep., National Cooperative
518 Highway Research Program, Bethlehem, Pennsylvania 1993.

519 [22] Gurney T. Fatigue of welded structures, 2nd Edition, Cambridge University Press,
520 Abington, Cambridge, UK, 1979.

521 [23] Zhang Y, Maddox S. Investigation of fatigue damage to welded joints under variable
522 amplitude loading spectra, Int J Fatigue:2009: 31 (1):138–152.

523 [24] Skorupa M. Load interaction effects during fatigue crack growth under variable
524 amplitude loading - a literature review. Part I: empirical trends," Fatigue & Fracture of
525 Engineering Materials & Structures. 1998; 21(8):987–1006.

526 [25] Skorupa M. Load interaction effects during fatigue crack growth under variable
527 amplitude loading - a literature review. Part II: qualitative interpretation," Fatigue &
528 Fracture of Engineering Materials & Structures. 1999; 22(10):905–926.

529 [26] Santecchia E, Hamouda AMS, Musharavati F, Zalnezhad E, Cabibbo M, El Mehtedi
530 M, Spigarelli S. A Review on Fatigue Life Prediction Methods for Metals. Advances in
531 Materials Science and Engineering. 2016; 2016:Article ID 9573524:1-26
532 http://dx.doi.org/10.1155/2016/9573524

533 [27] Ashish Aeran Sudath C., Siriwardane Ove Mikkelsen Ivar Langen A new nonlinear
534 fatigue damage model based only on S-N curve parameters. Int J Fatigue 2017;103: 327-
535 341.

536 [28] Claudio Baptista, AntonioReis, Alain Nussbaumer. Probabilistic S-N curves for
537 constant and variable amplitude. Int J Fatigue 2017;101(2): 312-327.
538 [29] Albrecht P, Yamada K. Simulation of service fatigue loads for short span highway
539 bridges, in: ASTM STP 671, Philadelphia, USA, 1979: 44
540 [30] Kumar H. Experimental investigation of fatigue life of friction stir welded 19501
541 aluminium T joint. M. Tech Thesis, G B Pant University of Agriculture and Technology,
542 Pantnagar, India, 2016.
543
544 [31] Birnbaum ZW, Saunders SC. A probabilistic interpretation of Miner's rule. SIAM
545 J Appl Math 1968;16(3):637–52
546 [32] Shimokawa T, Tanaka S. A statistical consideration of Miner's rule. Int J Fatigue
547 1980;4:165–70
548
549 [33] Rowatt JD, Spanos PD. Markov chain models for life prediction of composite
550 laminates. Struct Safe 1998;20:117–35.
551 [34] Doremus RH. Fracture statistics: a comparison of normal, Weibull and Type 1
552 Extreme value distribution, J Appl Phy, 1983;54: 193-198.